

Electron Cyclotron Maser Emission near the Cutoff Frequencies*

R. G. Hewitt and D. B. Melrose

School of Physics, University of Sydney,
Sydney, N.S.W. 2006.

Abstract

An earlier discussion of loss-cone driven cyclotron masers is extended to cover the case where the emission occurs close to the cutoff frequency of the o mode or the x mode. In general, wave growth may occur in one or two bands, and when two bands are allowed the lower band is close to the cutoff frequency. With the exception of the x mode at $s = 1$, growth in the lower band is allowed only for $\omega_p/\Omega_e > s$ and $\cos^2\theta > \frac{1}{2}$ for the o mode and for $\omega_p/\Omega_e > \{s(s-1)\}^{\frac{1}{2}}$ and $\cos^2\theta > (s-1)/s$ for the x mode, and growth in the lower band has no particularly favourable features when allowed. For the x mode at $s = 1$ both bands are allowed for all $\omega_p/\Omega_e \lesssim 1$ and growth in the lower band is possible over a wide range of angles in a very narrow frequency band. The spatial growth rate can be quite large due to the small group speed. However, the large spatial growth rate is offset by the short pathlengths for growth in a slowly spatially varying magnetic field due to the very narrow bandwidth of the growing waves. It is found that growth in the lower band is at best no more effective than growth in the upper band. We discuss the relative merits of growth in the two bands in a suggested application to terrestrial kilometric radiation. We also discuss cyclotron theories for type I solar radio emission, pointing out that our results do not favour such theories, and for solar microwave spike bursts.

1. Introduction

In an earlier paper (Hewitt *et al.* 1982; hereafter referred to as HMR), we discussed the properties of loss-cone driven electron cyclotron maser emission. In HMR we specifically excluded discussion of emission close to the cutoff frequencies of the x mode and the o mode. In the present paper we extend the discussion of HMR to these excluded cases, i.e. to emission in regions with refractive index $n = kc/\omega \ll 1$.

The main interest in growth near a cutoff frequency is associated with the possibility of large spatial growth rates due to small group speeds $v_g \ll c$. Here we are concerned with the possible importance of this effect for terrestrial (or auroral) kilometric radiation (TKR) and for certain solar radio emissions. For TKR the relevant growth is in the x mode at the fundamental $s = 1$. It has been noted by a number of authors (Omidi and Gurnett 1982; Melrose *et al.* 1982; Wu *et al.* 1982; Dusenbery and Lyons 1982; HMR) that growth in this case can occur close to the cutoff frequency, but this has not been explored in detail previously. Solar radio emissions for which cyclotron maser theories have been proposed include type I bursts (Twiss and Roberts 1958; Fung and Yip 1966; Mangeney and Veltri 1976) and microwave spike bursts

* Dedicated to the memory of Professor S. T. Butler who died on 15 May 1982.

(Holman *et al.* 1980; Melrose and Dulk 1982; Sharma *et al.* 1982). Observationally, the former is in the o mode and consists of short narrow-frequency bursts superimposed on a broadband continuum. Fung and Yip (1966) argued that the bursts could be due to what they referred to as a 'double frequency' solution, which is closely related to emission close to the cutoff frequency (see Section 2).

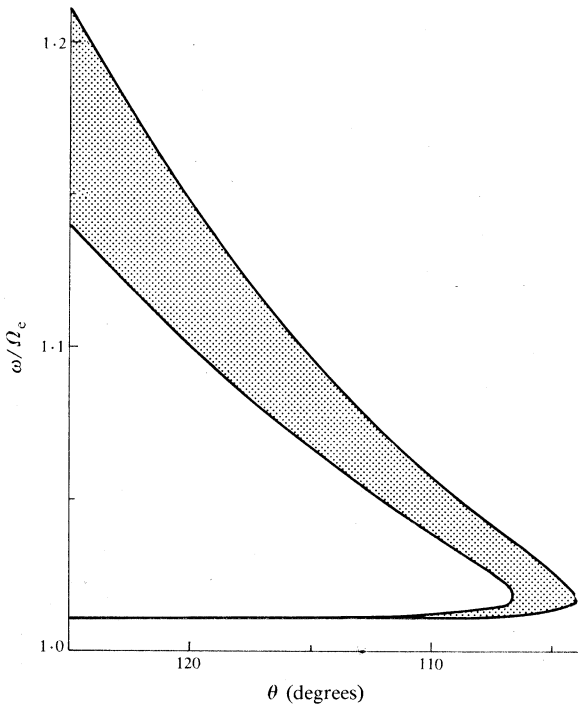


Fig. 1. Effective growth region (dotted area) for the x mode at $s = 1$ is plotted for $\omega_p/\Omega_e = 0.1$ as a function of ω and θ . (The parameters used are the same as those for Fig. 11a of HMR. The $V = 0$ curve coincides with the right-hand boundary.) The lower band is so narrow in frequency for $\theta \gtrsim 110^\circ$ that its bandwidth cannot be resolved here. Between the upper and the lower bands at fixed θ the growth rate is negative.

Another reason for considering emission near the cutoff frequency involves (a) the growth rate for $n = kc/\omega \ll 1$ and (b) the effect of refraction on the escaping radiation. The effect of refraction has been invoked in some cyclotron theories for Jupiter's decametric (DAM) radio emission; for example, by Ellis and McCulloch (1963) and by Goldstein and Eviatar (1979). We believe that the angular dependence of the maser operating at $kc/\omega \approx 1$ can account well for the inferred angular dependence of DAM (Hewitt *et al.* 1981) and that emission at $n \ll 1$ is not required for DAM. However, refraction may be important in solar microwave spike bursts, which seem particularly favourable for interpretation in terms of loss-cone driven cyclotron maser emission. A difficulty is that emission at $s = 1$ cannot escape through the second-harmonic absorption layer (where $\omega = 2\Omega_e$). To overcome this difficulty Melrose and Dulk (1982) suggested that the observed emission is at the second harmonic. An alternative possibility (Holman *et al.* 1980) is that the emission is at the fundamental and that when it reaches the second-harmonic absorption layer it is propagating nearly along the magnetic field; the absorption coefficient goes to zero at $\sin \theta = 0$ as $\sin^2 \theta$, leaving a 'window' at small θ through which the radiation can escape. The geometry seems to preclude $\theta \approx 0$ at the second-harmonic layer except if the maser operates close to the cutoff frequency, allowing emission at relatively small θ and allowing refraction to further decrease θ .

Although we have these various possible applications in mind, our main motivation is to explore the properties of growth near the cutoff frequency and to consider whether or not it can compete effectively with growth at $n \approx 1$. Growth at $n \ll 1$ can be important only if it has different properties from that at $n \approx 1$ and also if it can compete with growth at $n \approx 1$ for the available free energy.

We find it convenient to refer here to growth at $n \approx 1$ as being in the 'upper band' and that at $n \ll 1$ as being in the 'lower band'. As explained further below, this terminology arises from a consideration of the dependence of the growth rate on ω and θ (for $s\Omega_e$ less than the relevant cutoff frequency). On an ω - θ plot we find that, provided $|\theta - \frac{1}{2}\pi|$ is greater than some minimum value, growth at a given θ occurs in two frequency ranges separated by a range of ω where the waves are damped. The lower frequency band is very close to the cutoff frequency and has a very narrow bandwidth (an example is plotted in Fig. 1).

In Section 2 we describe the kinematics of the resonant interaction which allow maser emission close to the cutoff frequencies. Our detailed numerical results are presented in Section 3 and discussed in terms of a semiquantitative theory in Section 4. In Section 5 we discuss growth in the upper and lower band for the x mode at $s = 1$ in relation to the application to TKR, and in Section 6 we comment on the possible solar applications. The conclusions are summarized in Section 7.

2. Kinematics for Maser Action near the Cutoff Frequencies

The kinematic restrictions on cyclotron maser emission were developed in HMR in terms of the properties of the resonant ellipse in v_{\perp} - v_{\parallel} space. The condition $V^2 > 0$ for the ellipse to exist excludes a certain region of ω - θ space. The $V = 0$ curve is plotted in Figs 11a and 14 of HMR. However, before discussing this description of the kinematics, it is instructive to consider an alternative approach due to Ellis (1962) and Fung and Yip (1966).

The cutoff frequency of the o mode is at $\omega = \omega_p$, and the cutoff frequency for the x mode is at $\omega = \omega_x$ with

$$\omega_x = \frac{1}{2}\Omega_e + \frac{1}{2}(\Omega_e^2 + 4\omega_p^2)^{\frac{1}{2}}. \tag{1}$$

Ellis (1962) developed an electron cyclotron emission theory for DAM, and in discussing the kinematics for the emission he used a plot of n^2 versus ω . He plotted both the dispersion relation for the x mode, i.e. $n^2 = n_x^2(\omega, \theta)$, and also the Doppler condition for a single electron, i.e.

$$\omega - s\Omega_e(1 - \beta_{\perp}^2 - \beta_{\parallel}^2)^{\frac{1}{2}} - n\omega\beta_{\parallel} \cos \theta = 0 \tag{2}$$

for $s = 1$. At $n^2 = 0$ the Doppler curve (2) starts at the point $\omega = s\Omega_e(1 - \beta_{\perp}^2 - \beta_{\parallel}^2)^{\frac{1}{2}}$ and as ω tends to infinity the Doppler curves tend to a finite maximum value, which in practice is $\gg 1$. On the other hand, the dispersion curve for n^2 starts at the point $n^2 = 0$, $\omega = \omega_x$ and tends to $n^2 = 1$ as ω tends to infinity. It follows that for $s\Omega_e(1 - \beta_{\perp}^2 - \beta_{\parallel}^2)^{\frac{1}{2}} > \omega_x$ the two curves must cross at one and only one point, and for $s\Omega_e(1 - \beta_{\perp}^2 - \beta_{\parallel}^2)^{\frac{1}{2}} < \omega_x$ the two curves either intersect at two points or not at all. Hence a given electron resonates with only one wave at a given angle θ in the former case, and two or none in the latter case. Fung and Yip (1966) extended Ellis's graphical technique to include the o mode and higher harmonics. They called these two cases

'single' and 'double' frequency solutions respectively. The forbidden region in ω - θ space (cf. Figs 11*a* and 14 of HMR) corresponds to those ω and θ for which there are no values of v_{\perp} and v_{\parallel} for which the Doppler curve (2) intersects the relevant refractive index curve.

In the present case we are concerned with maser emission involving a distribution of electrons rather than a single electron. In place of (2) we have the kinematic requirement

$$k_{\parallel}^2 c^2 + s^2 \Omega_e^2 > \omega^2 \quad (3)$$

for the resonant ellipse to exist. By replacing the inequality in (3) by an equality and changing variables, the condition

$$n^2 = (\omega^2 - s^2 \Omega_e^2) / \omega^2 \cos^2 \theta \quad (4)$$

defines the boundary of the region where resonance is possible. On an n^2 - ω plot resonance is possible only to the left of the curve defined by (4).

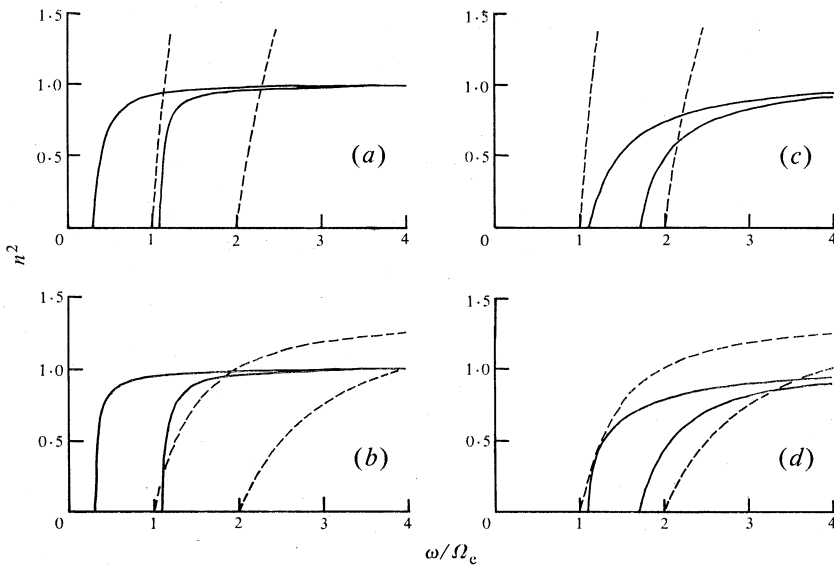


Fig. 2. Square of the refractive index as a function of ω/Ω_e for the o mode (left solid curve) and the x mode (right solid curve) above their respective cutoffs for (a) $\omega_p/\Omega_e = 0.3$ and $\theta = 120^\circ$; (b) $\omega_p/\Omega_e = 0.3$ and $\theta = 150^\circ$; (c) $\omega_p/\Omega_e = 1.1$ and $\theta = 120^\circ$; (d) $\omega_p/\Omega_e = 1.1$ and $\theta = 150^\circ$. Dashed curves are given by equation (4) with the same values of θ and with $s = 1$ (left) and $s = 2$ (right).

In Fig. 2 we plot the refractive index curves for the o mode and the x mode and the curve (4) for $s = 1$ and 2 for several different values of ω_p/Ω_e and $\cos \theta$. The following features are evident:

- (1) For $s\Omega_e$ greater than the cutoff frequency for the given mode, the curve (4) and the refractive index curve intersect at one and only one point for a given $\cos \theta$.
- (2) For $s\Omega_e$ less than the cutoff frequency the curves intersect at two points or not at all, depending on the value of $\cos \theta$.

(3) The x mode at $s = 1$ is exceptional due to $\Omega_e < \omega_x$ always being satisfied. In this case there can be zero or two intersection points, but never one.

(4) The boundary separating the regimes of zero and two intersection points corresponds to the two curves touching; this occurs for a particular value of $\cos^2\theta$ and two intersections occur only for $\cos^2\theta$ greater than the value so determined.

These properties have been deduced using (4), which corresponds to the resonant ellipse having a vanishing semimajor axis. For the x mode at $s = 1$ the curve $V = 0$ is plotted in ω - θ space in Fig. 14 of HMR, and the minimum value of $\cos^2\theta$ is determined by the position of the nose in this curve. The case of the x mode at $s = 1$ is discussed further in Section 4. For the other cases the condition for two intersection points to occur and the minimum value of $\cos^2\theta$ may be determined analytically, as shown in Appendix 1. The requirement that $s\Omega_e$ be less than the cutoff frequency leads to

$$\omega_p/\Omega_e > s, \quad \omega_p/\Omega_e > \{s(s-1)\}^{\frac{1}{2}} \quad (5a, b)$$

for the o mode and x mode respectively. The smallest possible value of $\cos^2\theta$ at which the two curves touch is when $s\Omega_e$ is equal to the cutoff frequency and the two curves are tangent to each other there. This leads to

$$\cos^2\theta > \frac{1}{2}, \quad \cos^2\theta > (s-1)/s \quad (6a, b)$$

for the o mode and the x mode respectively. Thus two intersection points occur for the o mode at $s = 1$ and the x mode at $s = 2$ only for $\omega_p > \Omega_e$ and $\omega_p > \sqrt{2}\Omega_e$, respectively, and for $\cos^2\theta > \frac{1}{2}$.

So far we have appealed only to the condition (4) for a resonance to be possible at all. As explained in HMR, effective growth is restricted to a small range of resonance ellipses which fit into and are approximately touching the boundary of the loss cone in v_{\perp} - v_{\parallel} space. For these ellipses we have $V > 0$ and then (4) is replaced by, for $\omega^2 \approx s^2\Omega_e^2$ and $V^2/c^2 \ll 1$,

$$n^2 = \frac{\omega^2 - s^2\Omega_e^2}{\omega^2 \cos^2\theta} + \frac{V^2}{c^2 \cos^2\theta}. \quad (7)$$

The centre of the resonance ellipse is at $(v_{\parallel}, v_{\perp}) = (v_c, 0)$ with, for $v_c^2/c^2 \ll 1$,

$$v_c/c = n \cos\theta. \quad (8)$$

The upper band for growth corresponds to $n \approx 1$ and $\cos\theta \approx v_c/c$ in equation (8) and to $(\omega^2 - s^2\Omega_e^2)/\omega^2 \cos^2\theta \approx 1 \gg V^2/c^2 \cos^2\theta$ in (7). For the lower band (7) and (8) are satisfied (for given favourable V and v_c) in a different way as discussed in detail in Section 4. For V much greater than the optimum value the resonant ellipses pass through regions of v_{\perp} - v_{\parallel} space where $\partial f/\partial v_{\perp}$ is negative, and these regions lead to negative contributions to the growth rate.

The separation of growth into two bands can be understood by fixing v_c and θ and considering how V varies with ω according to (7) and (8). One finds that the optimum values of V can be obtained either for $n^2 \approx (\omega^2 - s^2\Omega_e^2)/\omega^2 \cos^2\theta \approx 1 \gg V^2/c^2 \cos^2\theta$, which is the upper band, or near the cutoff frequency. In between, one can satisfy (7) and (8) only for much larger values of V which correspond to damping rather than growth. It is for this reason that the two bands in Fig. 1 are separated

by a region of damping. This effect is also apparent from the results of Omidi and Gurnett (1982) who found two growth bands (labelled I and III) separated by a band (labelled II) where damping occurs.

We are concerned here with the lower band. It is reasonably well defined by the vicinity of the lower of the intersections of the curve (4) with the refractive curve, as illustrated in Fig. 2. The lower band is characterized by frequencies close to the cutoff frequency, small refractive indices and narrow bandwidths.

3. Numerical Results

The numerical results reported here are for the distribution function defined by equations (11) and (12) of HMR. This is a hot Maxwellian distribution, with electron number density n_H and temperature T , with a hole at pitch angles $\alpha > \alpha_0$ and with the distribution falling off as $[\sin\{\frac{1}{2}(\pi - \alpha)\pi/(\pi - \alpha_0)\}]^N$ for $\alpha > \alpha_0 > \frac{1}{2}\pi$. Here we consider only the case $N = 6$.

Scaling

In HMR we chose $n_H = 10^{13} \text{ m}^{-3}$, $T = 10^8 \text{ K}$ and $\alpha_0 = 150^\circ$, and also $\Omega_e/2\pi = 3 \text{ GHz}$ and a cold electron density $n_C = 10^{15} \text{ m}^{-3}$. These parameters are appropriate to an application to solar microwave spike bursts (Melrose and Dulk 1982) but not to TKR or other possible situations of interest. However, as stated in HMR, the growth rate divided by Ω_e depends only on the ratios n_H/n_C , ω_p/Ω_e and ω/Ω_e . As a consequence our detailed results here and in HMR may be scaled to apply to other situations.

The growth rate depends on $n_C \propto \omega_p^2$ only implicitly through the dependence of the wave properties on ω_p/Ω_e . The choice of parameters stated above implies $\omega_p/\Omega_e = 0.1$. In considering different values of ω_p/Ω_e in HMR and here we are implicitly considering n_C to be the adjustable parameter.

From equations (11), (21) and (22) of HMR and equation (C4) of Melrose *et al.* (1982) the growth rate of the s th harmonic scales according to

$$\frac{\Gamma}{\Omega_e} = G \frac{n_H}{n_C} \left(\frac{\omega_p}{\Omega_e}\right)^2 \frac{c^2}{v_m^2} \sin \alpha_0 \left(\frac{v_m \sin \alpha_0}{c}\right)^{2s-2}, \quad (9)$$

with $v_m^2 \propto T$, and where G is a function of the dimensionless parameters ω/Ω_e , ω_p/Ω_e and N . Throughout we assume $n_H \ll n_C$ so that one has $\omega_p^2 \propto n_C$; we comment on this assumption in Section 5.

Results for x Mode at $s = 1$

The growth rate in the lower band for the x mode at $s = 1$ was calculated for the same range of ω_p/Ω_e as chosen in HMR when discussing growth in the upper band. The results are presented in Figs 3–8. Extremely small values of ω_p/Ω_e are excluded because they correspond to small resonant ellipses very close to the origin where absorption by the cold electrons cannot be neglected.

In Fig. 3 the maximum temporal growth rate is plotted as a function of θ . As expected growth occurs only for $|\cos \theta|$ greater than some minimum value which increases with ω_p/Ω_e . However, unlike in the upper band, the growth rate is insensitive to the value of θ above this minimum. The dependence of the growth rate on ω_p/Ω_e

involves a rapid rise with $\omega_p/\Omega_e \lesssim 0.10$, reaching a maximum at $\omega_p/\Omega_e \approx 0.15$ followed by a decrease at $\omega_p/\Omega_e \gtrsim 0.15$. The value of the maximum growth rate in the lower band, i.e. for $\omega_p/\Omega_e \approx 0.15$, is comparable with the maximum growth rate in the upper band at the same value of $\omega_p/\Omega_e \approx 0.15$ (and at the most favourable angle), cf. Fig. 13a of HMR. A semiquantitative interpretation of these features is developed in Section 4.

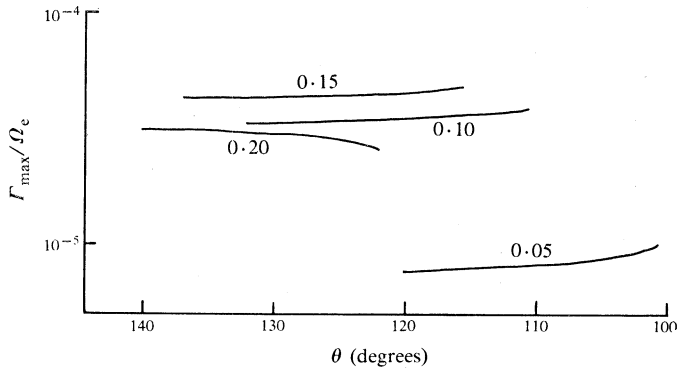


Fig. 3. Maximum relative temporal growth rate Γ_{\max}/Ω_e in the lower band $s = 1$ x mode as a function of θ for the four values of ω_p/Ω_e indicated.

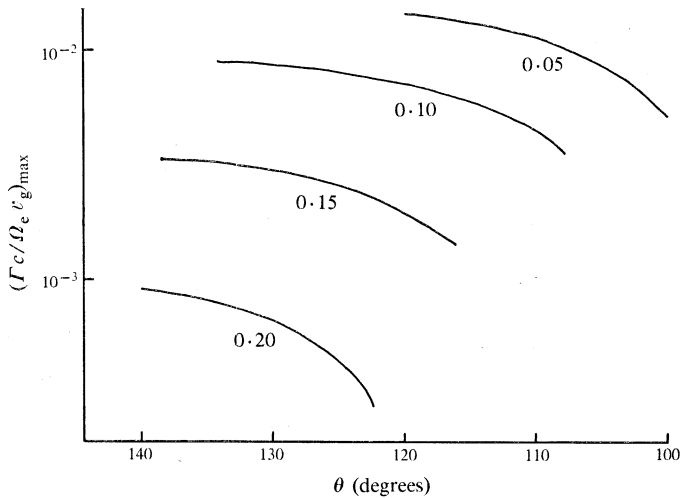


Fig. 4. Maximum relative spatial growth rate $(\Gamma c/\Omega_e v_g)_{\max}$ in the lower band $s = 1$ x mode as a function of θ for the same four values of ω_p/Ω_e as in Fig. 3.

The spatial growth rate is equal to the temporal growth rate divided by the group speed v_g . The spatial growth rate is plotted in Fig. 4 for the same parameters as in Fig. 3. It increases as ω_p/Ω_e decreases, and this is due to a rapid decrease in v_g as ω_p/Ω_e decreases. The strong dependence of v_g on ω_p/Ω_e is due to the difference between the frequency range in which amplification occurs and the cutoff frequency being a sensitive function of ω_p/Ω_e . This is illustrated in Fig. 5 where the differences

$(\omega - \omega_x)/\Omega_e$ are plotted for the frequencies at which the growth rate is half its maximum value. It is shown in Appendix 2 that, for $\omega \approx \omega_x$, v_g varies with ω as $(\omega - \omega_x)^{\frac{1}{2}}$ for the x mode, and hence one infers that v_g/c is of order $\{(\omega - \omega_x)/\Omega_e\}^{\frac{1}{2}}$ for $\omega \approx \omega_x$. Thus the strong dependence of the spatial growth rate on ω_p/Ω_e is ultimately due to the frequency of emission approaching the cutoff frequency rapidly with decreasing ω_p/Ω_e and hence causing the group speed to approach zero.

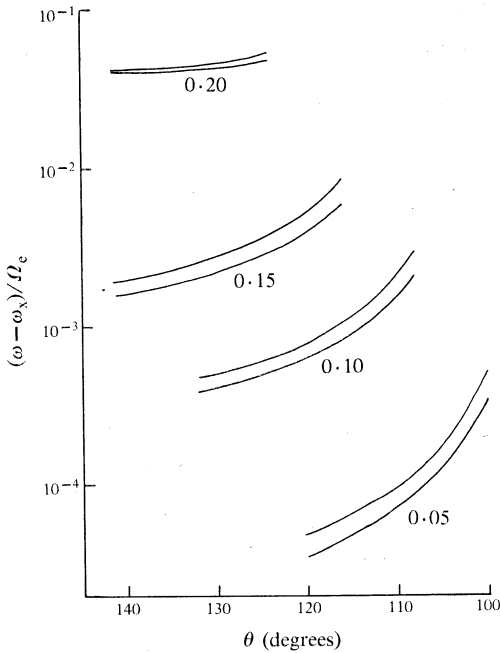
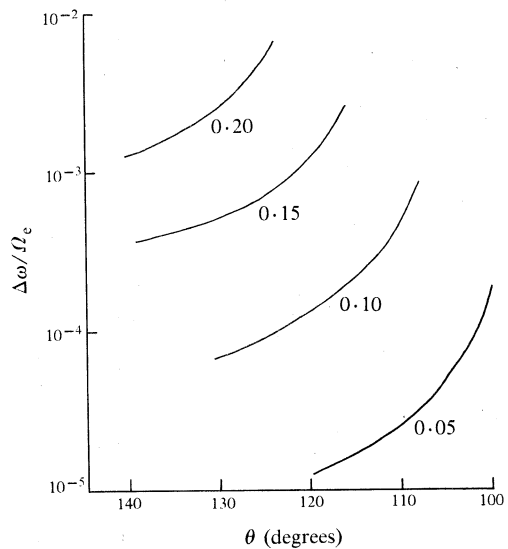


Fig. 5. Relative differences $(\omega - \omega_x)/\Omega_e$ between the frequencies at which the spatial growth rate in the lower band $s = 1$ x mode is half its maximum value and the cutoff frequency as a function of θ for the same values of ω_p/Ω_e as in Fig. 3.

Fig. 6. Relative effective bandwidth $\Delta\omega/\Omega_e$ of the lower band $s = 1$ x mode as a function of θ for the same values of ω_p/Ω_e as in Fig. 3.



The difference between the two curves in each pair in Fig. 5 defines an effective bandwidth for the growing waves. This bandwidth is plotted in Fig. 6; it decreases rapidly with decreasing ω_p/Ω_e . Hence, at small values of ω_p/Ω_e , we have quite large spatial growth rates, but the growing waves are restricted to a very narrow bandwidth.

The effectiveness of amplification depends on the optical depth for amplification, which is equal to the maximum possible number of e-folding growths. We may estimate this optical depth by multiplying the spatial growth rate by the pathlength over which amplification can occur. This pathlength is limited by the restriction that Ω_e must change by less than the bandwidth of the growing waves. Thus the maximum pathlength for amplification may be estimated from the ratio of the bandwidth of the growing waves to $|\text{grad } \Omega_e|$. There is an additional geometric factor which could be taken into account: the pathlength for amplification is inversely proportional to the cosine of the angle between v_g and $\text{grad } \Omega_e$. We discuss this geometric factor in Appendix 2 where we argue that it is unlikely that its effect is large.

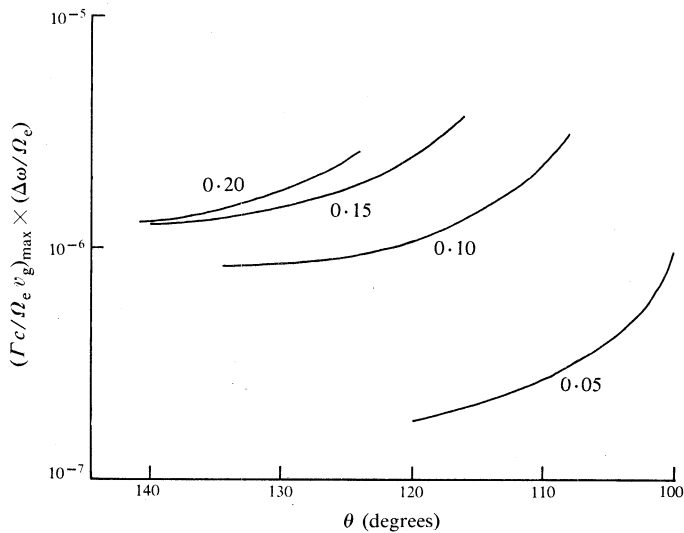


Fig. 7. Product of the relative spatial growth rate and the relative effective bandwidth of the lower band $s = 1 \times$ mode as a function of θ for the same values of ω_p/Ω_e as in Fig. 3.

In Fig. 7 we plot the product of the spatial growth rate times the bandwidth of the growing waves; this product is proportional to the maximum optical depth for amplification. From Fig. 7 one infers that the optical depth decreases with decreasing ω_p/Ω_e . Thus, contrary to what the dependence of the spatial growth rate on ω_p/Ω_e would suggest, amplification becomes less and less effective as ω_p/Ω_e is decreased. The results, plotted in Fig. 7 also suggest that amplification is most effective at the smallest allowed values of $|\cos \theta|$. The optimum values are $\omega_p/\Omega_e \approx 0.15$ and $|\cos \theta| \approx 0.45$. In Section 4 we discuss how these optimum values should depend on the assumed values of α_0 and T .

The resonant ellipses at which the maximum growth occurs for different values of ω_p/Ω_e are illustrated in Fig. 8. A notable feature is that the size of the ellipses

decreases with decreasing ω_p/Ω_e . Specifically, the ellipses are nearly circles, and the radius of the circle and the distance of its centre from the origin are roughly proportional to ω_p/Ω_e . One feature not shown in Fig. 8 is that the ellipses are roughly independent of θ over a wide range above the minimum allowed value of $|\cos \theta|$. This is in contrast to the sharp dependence on θ of the ellipses for growth in the upper band; this sharp dependence may be regarded as the cause for the growth being restricted to the surface of a hollow cone (see e.g. Hewitt *et al.* 1981 and HMR).

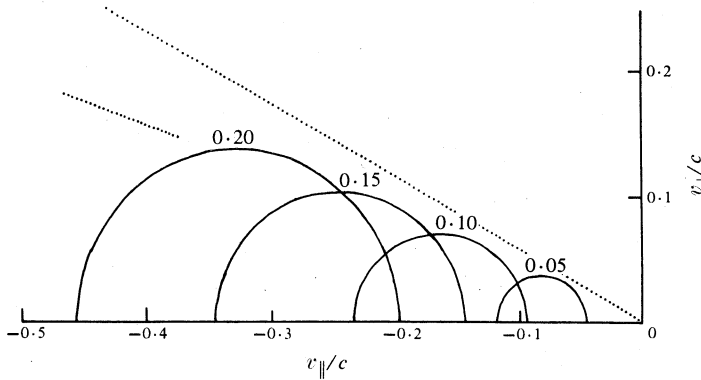


Fig. 8. Resonant ellipses for maximum spatial growth rates in the lower band $s = 1$ x mode for the four values of ω_p/Ω_e indicated. These ellipses are essentially independent of θ .

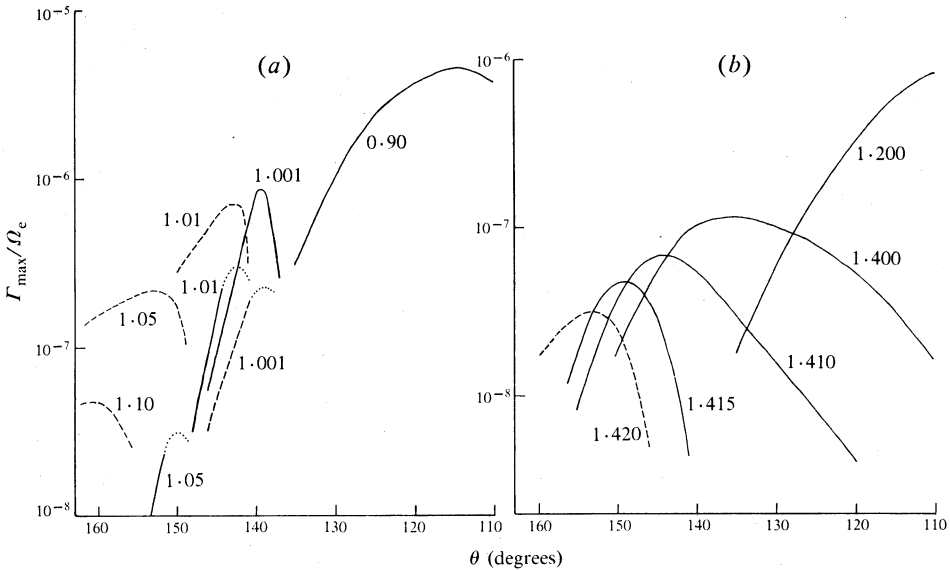


Fig. 9. Maximum relative temporal growth rate Γ_{\max}/Ω_e in (a) the $s = 1$ o mode and (b) the $s = 2$ x mode as a function of θ for the values of ω_p/Ω_e indicated. In (a), for values of $\omega_p/\Omega_e > 1$, growth can occur in both the upper band (solid curves) and the lower band (dashed curves). The dotted sections of the curves for the more weakly growing band are schematic. In (b), growth in both bands can occur when $\omega_p/\Omega_e > 1.414$; growth rates in the bands are comparable only for a narrow range of values of ω_p/Ω_e near 1.417.

As pointed out above, very small values of ω_p/Ω_e have been excluded from our discussion. The reason is that the resonant ellipse for $\omega_p/\Omega_e = 0.01$ is so close to the origin (cf. Fig. 8) that we cannot neglect damping by thermal electrons, as pointed out in connection with Table 2 of HMR. Another reason is that the form of the loss cone we have chosen, specifically $\alpha > \alpha_0$ independent of v_{\perp} , is over-idealized and in practice the loss cone disappears below some value of v (see e.g. Croley *et al.* 1978). A further problem with very small values of ω_p/Ω_e is that the contribution of the hot electrons to the dispersion of the waves cannot be neglected, specifically for $n_H \approx n_C$. This final point is discussed further in Section 5.

Growth for o Mode at $s = 1$ and x Mode at $s = 2$

As shown in Section 2 growth very close to the cutoff frequency is possible for the o mode at $s \geq 1$ and for the x mode at $s \geq 2$, but only under special circumstances. In Fig. 9 we plot the growth rates for (a) the o mode at $s = 1$ and (b) the x mode at $s = 2$ for ranges of ω_p/Ω_e which include the regions identified in Section 2, specifically by equations (5) and (6). It is clear that the growth rates near the cutoff frequencies in these cases are very much smaller than for more favourable choices of parameters. There seems no plausible situation in which growth in the lower band would be important for the o mode or for the x mode at $s \geq 2$.

4. Interpretation

In Section 6 of HMR we developed a semiquantitative theory which describes most of the properties of the loss-cone driven maser. Here we extend that theory to account for the additional features found above for growth at $s = 1$ and 2 of the x mode and at $s = 1$ of the o mode just above their cutoff frequencies.

The features requiring explanation for the x mode at $s = 1$ include:

- (i) The temporal growth rate is roughly independent of $\cos \theta$ for $|\cos \theta|$ greater than a minimum value which decreases with decreasing ω_p/Ω_e .
- (ii) Growth occurs in a range of values of $(\omega - \omega_x)/\Omega_e$ which decreases very rapidly with decreasing ω_p/Ω_e below some optimum value, which is $\omega_p/\Omega_e \approx 0.15$ here.
- (iii) The resonant ellipse corresponding to maximum growth has its semimajor axis V and the distance v_c of its centre from the origin roughly proportional to $\omega_p/\Omega_e \lesssim 0.15$.
- (iv) This resonant ellipse is insensitive to the value of $\cos \theta$ above the minimum for $|\cos \theta|$ mentioned in (i).

The features requiring explanation in the other cases include:

- (v) Growth of the o mode at $s = 1$ is possible near the cutoff frequency only for $\omega_p \gtrsim \Omega_e$ and $\cos^2 \theta \gtrsim \frac{1}{2}$; the maximum growth rate is much smaller than in the case $\omega \approx \Omega_e \gg \omega_p$.
- (vi) Growth of the x mode at $s = 2$ is also possible near the cutoff frequency for $\omega_x \gtrsim 2\Omega_e$ and $\cos^2 \theta \gtrsim \frac{1}{2}$; the maximum growth rate in this case is also much smaller than for $\omega \approx 2\Omega_e \gg \omega_x$.

Minimum Value of $|\cos \theta|$

The value of $|\cos \theta|$ below which growth of the x mode at $s = 1$ is not possible is implied by an argument given in Section 6 of HMR. The boundary curve $V = 0$

in Fig. 14 of HMR does not extend to values of $|\cos \theta|$ less than about $2\omega_p/\Omega_e$, as implied in equation (19b) of HMR. Growth corresponds to an ellipse with $V > 0$ and must be restricted to $|\cos \theta|$ larger than $2\omega_p/\Omega_e$. Inspection of Fig. 3 in Section 3 suggests that

$$|\cos \theta| \gtrsim 4\omega_p/\Omega_e \quad (10)$$

is a reasonable estimate of the minimum value of $|\cos \theta|$ for ω_p/Ω_e much less than the optimum value of ≈ 0.15 . The inequality (10) is consistent with the semiquantitative theory of HMR.

Dependence of Resonant Ellipse on ω and θ

Now consider the properties of the resonant ellipses for the x mode at $s = 1$. The ellipses are nearly circular and may be described in terms of the parameters v_c and V specifying their centres ($v_{\parallel} = v_c$, $v_{\perp} = 0$) and semimajor axes ($v_{\perp} \leq V$). From the results of HMR, in the semirelativistic approximation, we have

$$v_c/c = n \cos \theta, \quad (11)$$

$$V/c = \{(v_c/c)^2 - 2(\omega - \Omega_e)/\Omega_e\}^{\frac{1}{2}}, \quad (12)$$

and near the cutoff frequency for the x mode we have

$$n^2 = 2(\omega - \omega_x)/(\omega - \Omega_e)(1 + \cos^2 \theta). \quad (13)$$

Favourable ellipses for growth due to a loss-cone distribution have $V \approx |v_c| \sin \alpha_0 \ll |v_c|$. Hence in (12) we require

$$v_c^2/c^2 \approx 2(\omega - \Omega_e)/\Omega_e. \quad (14)$$

The approximation (13) applies for $\omega - \omega_x \lesssim \omega_p^2/\Omega_e$, when we have $\omega - \Omega_e \approx \omega_x - \Omega_e \approx \omega_p^2/\Omega_e$ to within a factor of 2. Then (11), (13) and (14) imply

$$\frac{\omega - \omega_x}{\Omega_e} \approx \left(\frac{\omega - \Omega_e}{\Omega_e}\right)^2 \frac{1 + \cos^2 \theta}{\cos^2 \theta} \approx \left(\frac{\omega_p}{\Omega_e}\right)^4 \frac{1 + \cos^2 \theta}{\cos^2 \theta}. \quad (15)$$

Moreover, on inserting (15) in (13) and thence in (11), one finds

$$|v_c/c| \approx \sqrt{2} \omega_p/\Omega_e. \quad (16)$$

The result (16) with $V \approx |v_c| \sin \alpha_0$ accounts for property (iii) listed at the beginning of this section, namely that the size of the resonant ellipse is proportional to ω_p/Ω_e . It also accounts for property (iv), namely that the properties of the resonant ellipse are roughly independent of $\cos \theta$.

Property (ii) implies that the value of $(\omega - \omega_x)/\Omega_e$ at which maximum growth occurs decreases rapidly with decreasing ω_p/Ω_e . According to (15) this variation should be as the fourth power of $\omega_p/\Omega_e \ll 0.15$. Inspection of Fig. 5 shows that our numerical results are consistent with a variation of $(\omega - \omega_x)/\Omega_e$ as the fourth power of ω_p/Ω_e .

It may be concluded that our semiquantitative theory accounts for the properties (i)–(iv) for growth of the x mode at $s = 1$ near the cutoff frequency.

The o Mode at $s = 1$ and x Mode at $s = 2$

In the other cases considered, namely the o mode at $s = 1$ and the x mode at $s = 2$, growth near the cutoff frequency is possible only for a very restricted range of the parameter ω_p/Ω_e , and even when possible it is quite weak. Inspection of our numerical results shows that the underlying reason is that the resonant ellipses are much larger than is favourable. That is, the allowed value of v_c and V place the ellipse at such high values of v that there are few electrons to drive the instability.

To see why the ellipses are moderately large consider the requirement $V^2 \ll v_c^2$ for a loss-cone distribution. For both $V^2, v_c^2 \ll c^2$ we have, from equations (7) and (8),

$$\frac{V^2}{c^2} = \frac{v_c^2}{c^2} - \frac{\omega^2 - s^2\Omega_e^2}{\omega^2}, \quad \frac{v_c^2}{c^2} = n^2 \cos^2 \theta. \quad (17a, b)$$

For $s\Omega_e > \omega_c$, where $\omega_c = \omega_p$ or ω_x is the cutoff frequency, $V < v_c$ requires $\omega > s\Omega_e > \omega_c$, which precludes emission arbitrarily close to the cutoff frequency. This places a lower limit on n^2 and hence on v_c^2 . For $s\Omega_e < \omega_c$ we require $\omega > \omega_c > s\Omega_e$ and then the term $\omega^2 - s^2\Omega_e^2$ cannot be arbitrarily small. In this case there is a lower limit on the final term in (17a) and hence on v_c^2 in order for V^2 to be positive. In brief, one concludes that the condition $v_c^2/c^2 \approx (\omega^2 - s^2\Omega_e^2)/\omega^2 \gg V^2/c^2$ implied by $V^2 \ll v_c^2$ in (17a) precludes values of ω very close to $s\Omega_e$ and hence very close to the cutoff frequency.

Although this discussion does not rule out growth of the o mode at $s = 1$ and the x mode at $s = 2$ near cutoff from ever being important, it imposes another severe constraint. Already in Section 2 we inferred that the growth is restricted to a very small range of ω_p/Ω_e and is restricted also in angle. The foregoing discussion suggests that it could be favourable only if the resonant ellipses implied by the kinematic restrictions occur in a region of velocity space with a large value of $\partial f/\partial v_\perp$. We have not explored this point systematically, but our results suggest that one requires electrons with $\beta \gtrsim 0.1$, for example, an energy of several keV. Even if this additional condition is satisfied, we would not expect the growth to be important for $s \geq 2$. The reason is that the growth rate is proportional to n^{2s-2} , and growth at small n is intrinsically unfavourable for $s \geq 2$.

5. Application to TKR

The suggestion that the terrestrial kilometric radiation is due to a loss-cone driven cyclotron maser has received wide support recently (Wu and Lee 1979; Omidi and Gurnett 1982; Wu *et al.* 1982; Melrose *et al.* 1982; Dusenbery and Lyons 1982). However, it is not clear whether growth in the upper or lower bands is the more favourable. A related point is the neglect of the contribution of the hot electrons to the dispersion in the lower band. In this section we restrict our discussion to these two points.

Apart from our work here and in HMR, calculations relevant to the comparison between the upper and lower bands for growth of the x mode at $s = 1$ have been presented by Omidi and Gurnett (1982) and Wu *et al.* (1982). However, neither set of calculations provides a clear answer to which band is the more favourable. Omidi and Gurnett calculated the growth rate for a fixed $\theta = 100^\circ$ and for $\omega_p/\Omega_e = 0.05$. They used a distribution function calculated from S3-3 data (see e.g. Croley *et al.*

1978). It is pertinent to point out that the contours provided from the S3-3 data involve considerable interpolation and, of more relevance, the distribution does not have a pure loss cone. These features could account for Omidi and Gurnett finding a greater temporal growth rate in the lower band than in the upper band, in disagreement with the results presented here and in HMR. Wu *et al.* calculated the temporal growth rate at fixed values of θ . Most of their calculations corresponded to values of θ which exclude the upper band. The exceptions are for their model C which included no cold electrons. They found growth for $\theta = 90^\circ$ to be the most favourable in this case, but cautioned that their result for $\theta = 90^\circ$ may be unreliable because their distribution function contains a loss cone in the downward as well as in the upward direction and the resonant ellipses pass through both. (According to arguments in HMR the case $\theta = 90^\circ$ is kinematically forbidden.) Moreover, the case where there is no cold plasma is a special one; we return to this point in the next subsection. In brief, the Omidi and Gurnett calculation of the growth rates for the two bands may not be relevant to a pure loss cone and Wu *et al.* (1982) did not explore the upper band adequately.

The results found here and in HMR do not lead to a clear indication as to whether emission in the upper or the lower band is to be preferred. The important parameter is the spatial growth rate times the bandwidth of the growing waves. According to Figs 2, 12a and 13a of HMR the maximum value of $(\Gamma c/\Omega_e v_g)(\Delta\omega/\Omega_e)$ for the upper band is between 10^{-5} and 10^{-6} , which coincides with the maximum value of the relevant parameter for the lower band according to Fig. 7 in Section 3 above. Growth in the upper band leads to emission over a narrow range of angles and frequencies, and growth in the lower band leads to emission over a broad range of angles and an extremely narrow range of frequencies. Wu *et al.* (1982) suggested that the evidence for the radiation pattern for TKR being a filled cone (Green *et al.* 1977), rather than on the surface of a hollow cone as for DAM, tends to favour emission in the lower band. This is a valid argument, but not a compelling one because scattering or specular reflections off locally higher density structures in the source region could allow a strongly angle-dependent emission mechanism to lead to escaping radiation over a broad range of angles.

We conclude that neither existing calculations, including our own, nor physical arguments lead to a strong case for preferential growth in either the upper or lower bands. We favour growth in the upper band, as stated in HMR, primarily because growth in the lower band is as favourable only for a restricted range of ω_p/Ω_e . The actual value of ω_p/Ω_e in the source region is not well determined, and it could be very low. Very low values of ω_p/Ω_e lead to the possibility of an alternative version of the cyclotron instability.

Effect of Very Low Cold Plasma Density

Our calculations have been performed assuming that the number density of the hot electrons with the loss-cone distribution is much less than that of the cold electrons. Throughout, the parameter ω_p includes only the contribution of the cold (C) electrons, and the actual value of the plasma frequency for the hot (H) electrons alone corresponds to $\omega_{pH}/\Omega_e = 10^{-2}$ in our numerical work. Consequently, our results are invalid for $\omega_p/\Omega_e \lesssim 10^{-2}$. Wu *et al.* (1982) pointed out that the case when cold electrons are neglected (their case C) is a relatively favourable one. When the

cold plasma density is low enough the nature of the instability changes. It has been shown by Winglee (1983) that the instability under consideration here, which he calls the Wu and Lee instability following Wu and Lee (1979), passes over into an azimuthal bunching instability which is important in laboratory gyrotrons (Sprangle and Drobot 1977; Chu and Hirshfield 1978). Winglee found that if $n_c \lesssim n_H$ then both the Wu and Lee and the azimuthal bunching instabilities could be present simultaneously; then the azimuthal bunching instability occurs over a broad range of angles at $kc/\omega \ll 1$ and the Wu and Lee instability occurs at $0.1 \lesssim kc/\omega \lesssim 1$. Growth in the Wu *et al.* (1982) case C is of this type, as is shown by the fact that the emission can occur below the (nonrelativistic) cyclotron frequency.

Although our theory breaks down for $\omega_p/\Omega_e \lesssim 10^{-2}$, cyclotron emission is not excluded in this regime. A different type of cyclotron instability simply takes over for loss-cone distributions with $n_H \approx n_c$ and low values of ω_p/Ω_e .

6. Cyclotron Theories for Solar Radio Emissions

Now let us comment on the suggested applications to type I solar radio bursts and the solar microwave spike bursts.

Twiss and Roberts (1958) suggested that type I solar radio emission might be due to cyclotron maser emission. This idea was analysed in detail by Fung and Yip (1966). In their theory type I bursts, as opposed to the type I continuum, come from emission at a 'double frequency' solution, which is closely related to emission close to the cutoff frequency as considered here; specifically, it requires $\omega_p - s\Omega_e \ll \omega_p$ for emission at the s th harmonic. A later form of the cyclotron theory is that due to Mangeney and Veltri (1976). The main difficulty with cyclotron theories is that type I emission is strongly polarized in the sense of the o mode, whereas cyclotron emission favours the x mode.

Although the foregoing theories did not invoke a loss-cone driven maser, the question arises as to whether such a theory might be favourable, especially in view of more recent theories for type I emission which involve loss-cone driven instabilities producing Langmuir waves (see e.g. Melrose 1977, 1980a; Benz and Wentzel 1981). Dulk and Melrose (1983) argued that such a cyclotron emission is unfavourable. Their reason is that there is a relatively narrow range of the parameter ω_p/Ω_e over which growth of the o mode is preferred, especially for $0.3 \lesssim \omega_p/\Omega_e \lesssim 1$, and this range is not thought appropriate for type I sources. This argument is further strengthened by our discussion here of growth near the cutoff frequency for the o mode. The possibility, for example, as suggested by Fung and Yip (1966), that growth near the cutoff frequency may be particularly favourable for the interpretation of certain features of type I emission is not supported by our results.

The suggestion that solar microwave bursts might be due to fundamental emission near the cutoff frequency of the x mode seems a possible alternative to emission at the second harmonic (Melrose and Dulk 1982). The restriction to $|\theta - \frac{1}{2}\pi| \ll 1$ for the upper band does not apply to the lower band (cf. Fig. 4), and emission at moderate θ can occur with refraction causing a further decrease in θ . This may allow some of the radiation to arrive at the second-harmonic absorption layer at sufficiently small θ for it to pass through the small- θ window, as suggested by Holman *et al.* (1980). A detailed model involving ray tracing is needed to discuss this point quantitatively. A basic difficulty remains: if growth in the upper band is faster than that in the lower band, then virtually all the free energy should go into the upper band before the lower

has time to grow significantly. A related difficulty is relevant to the production of the second harmonic, as proposed by Melrose and Dulk (1982): growth at the second harmonic must compete with faster growing fundamental x mode or o mode radiation except for a small range of ω_p/Ω_e between about 1 and 1.4. It is not clear whether the observed emission escapes because it is generated at the second (or higher) harmonic or because it is fundamental emission which arrives at the second-harmonic absorption layer at small θ .

7. Conclusions

We have explored loss-cone cyclotron emission at close to the cutoff frequencies for the x mode at $s = 1$ and 2 and for the o mode at $s = 1$. Except for the x mode at $s = 1$, the region close to the cutoff frequency is not particularly favourable, and it is distinctly unfavourable in the sense that emission there is allowed only for special values of the parameter ω_p/Ω_e , as given by equations (5).

Growth of the x mode at $s = 1$ is possible in two bands for all $\omega_p/\Omega_e < 1$. We refer to these as the upper and lower bands. Growth in the upper band was discussed by HMR: it is restricted to a narrow range of angles and a narrow range of frequencies. It has been shown here that growth in the lower band occurs over a relatively broad range of angles and an extremely narrow frequency range. The semiquantitative theory developed in Section 6 of HMR has been extended in Section 4 here to include the properties of emission in the lower band.

The work of several authors might be interpreted as suggesting a preference for growth near the cutoff frequency in the interpretation of TKR (see e.g. Omidi and Gurnett 1982; Wu *et al.* 1982; Dusenbery and Lyons 1982). However, until now there has not been a detailed comparison of growth in the upper and lower bands. Our investigation leads us to favour growth in the upper band, but we cannot rule out growth in the lower band. The effective number of growth lengths is comparable under the most favourable circumstances for the lower band (otherwise the upper band dominates). It may well be that growth in both bands occurs. One would then expect TKR to show a double banded structure, with both bands being close to the gyrofrequency. There is some evidence for such a double banded structure in spectra reported by Benson (1982).

References

- Benson, R. F. (1982). *Geophys. Res. Lett.* **9**, 1120.
 Benz, A. O., and Wentzel, D. G. (1981). *Astron. Astrophys.* **94**, 100.
 Chu, K. R., and Hirshfield, J. L. (1978). *Phys. Fluids* **21**, 461.
 Croley, D. R., Jr, Mizera, P. F., and Fennell, J. F. (1978). *J. Geophys. Res.* **83**, 2701.
 Dulk, G. A., and Melrose, D. B. (1983). In 'Solar Noise Storms' (Eds A. O. Benz and P. Zlobec), p. 219 (Osservatorio Astronomico di Trieste: Trieste).
 Dusenbery, P. B., and Lyons, L. R. (1982). *J. Geophys. Res.* **87**, 7476.
 Ellis, G. R. A. (1962). *Aust. J. Phys.* **15**, 344.
 Ellis, G. R. A., and McCulloch, P. M. (1963). *Aust. J. Phys.* **16**, 380.
 Fung, P. C. W., and Yip, W. K. (1966). *Aust. J. Phys.* **19**, 759.
 Goldstein, M. L., and Eviatar, A. (1979). *Astrophys. J.* **230**, 261.
 Green, J. L., Gurnett, D. A., and Shawhan, S. D. (1977). *J. Geophys. Res.* **82**, 1825.
 Hewitt, R. G., Melrose, D. B., and Rönmark, K. G. (1981). *Proc. Astron. Soc. Aust.* **4**, 221.
 Hewitt, R. G., Melrose, D. B., and Rönmark, K. G. (1982). *Aust. J. Phys.* **35**, 447.
 Holman, G. D., Eichler, D., and Kundu, M. R. (1980). In 'Radio Physics of the Sun' (Eds M. R. Kundu and T. E. Gergely), p. 457 (Reidel: Dordrecht).

Mangeny, A., and Veltri, P. (1976). *Astron. Astrophys.* **47**, 165; 181.
 Melrose, D. B. (1977). *Radiophys. Quant. Electron.* **20**, 945.
 Melrose, D. B. (1980a). *Sol. Phys.* **67**, 357.
 Melrose, D. B. (1980b). 'Plasma Astrophysics', Vol. II (Gordon and Breach: New York).
 Melrose, D. B., and Dulk, G. A. (1982). *Astrophys. J.* **259**, 844.
 Melrose, D. B., Rönnmark, K. G., and Hewitt, R. G. (1982). *J. Geophys. Res.* **87**, 5140.
 Omid, N., and Gurnett, D. A. (1982). *J. Geophys. Res.* **87**, 2377.
 Omid, N., Wu, C. S., and Gurnett, D. A. (1983). Generation of auroral kilometric and Z-mode radiation by the cyclotron maser mechanism. *J. Geophys. Res.* (in press).
 Sharma, R. R., Vlahos, L., and Papadopoulos, K. (1982). *Astron. Astrophys.* **112**, 377.
 Sprangle, P., and Drobot, A. T. (1977). *IEEE Trans. Microwave Theory Tech.* **25**, 528.
 Twiss, R. Q., and Roberts, J. A. (1958). *Aust. J. Phys.* **11**, 424.
 Winglee, R. M. (1983). *Plasma Phys.* **25**, 217.
 Wu, C. S., and Lee, L. C. (1979). *Astrophys. J.* **230**, 621.
 Wu, C. S., Wong, H. K., Gorney, D. J., and Lee, L. C. (1982). *J. Geophys. Res.* **87**, 4476.

Appendix 1. Intersection of Curves $n^2 = n_\sigma^2$ and $V = 0$

The curve of equation (4), namely

$$n^2 = (\omega^2 - s^2\Omega_e^2)/\omega^2 \cos^2\theta, \tag{A1}$$

and the refractive index curve $n^2 = n_\sigma^2(\omega, \theta)$ for either mode ($\sigma = 1$ for the o mode, $\sigma = -1$ for the x mode) intersect at two points only for $s\Omega_e$ less than the respective cutoff frequency and $\cos^2\theta$ greater than a minimum value. This minimum may be determined by setting $s\Omega_e$ equal to the cutoff frequency and requiring that the slopes $\partial n^2/\partial\omega$ at $n^2 = 0$ of the two curves be equal. From equation (A1) we have

$$[\omega \partial n^2/\partial\omega]_{n^2=0} = 2/\cos^2\theta. \tag{A2}$$

For the refractive index curves we use the following formulae (see Melrose 1980b; p. 261):

$$n_\sigma \frac{\partial(\omega n_\sigma)}{\partial\omega} = 1 + \frac{XYT_\sigma \cos\theta}{2(T_\sigma - Y \cos\theta)^2} \left(1 + \frac{1+X}{1-X} \frac{1-T_\sigma^2}{1+T_\sigma^2} \right), \tag{A3}$$

$$T_\sigma = -1/T_{-\sigma} = \frac{-\frac{1}{2}Y^2 \sin^2\theta - \sigma \{ \frac{1}{4}Y^4 \sin^4\theta + (1-X)^2 Y^2 \cos^2\theta \}^{\frac{1}{2}}}{Y(1-X) \cos\theta}, \tag{A4}$$

with $Y \equiv \Omega_e/\omega$ and $X \equiv \omega_p^2/\omega^2$ and with $\omega = s\Omega_e = \omega_p$ for the o mode and $\omega = s\Omega_e = \omega_x$ for the x mode. For the o mode we set $X = 1$ at the cutoff frequency implying $T_o = \infty$ except in $(1-X)T_o = -Y \sin^2\theta/\cos\theta$, and then (A3) gives

$$[\omega \partial n_o^2/\partial\omega]_{n_o^2=0} = 2/\sin^2\theta. \tag{A5}$$

For the x mode the cutoff occurs at $1-X = Y$ when one has $T_x = \cos\theta$, and then (A3) with $1-X = Y = 1/s$ implies

$$[\omega \partial n_x^2/\partial\omega]_{n_x^2=0} = 2(2s-1)/(s-1)(1+\cos^2\theta). \tag{A6}$$

Equating (A5) and (A6) to (A2) leads to the minimum values of $\cos^2\theta$ implied by (6a) and (6b) respectively.*

* Note that in formula (8c) of HMR we have inadvertently omitted a factor of $\cos\theta/|\cos\theta|$ in the expression for T_σ : in (8c) σ should be replaced by $\sigma \cos\theta/|\cos\theta|$.

Appendix 2. Group Velocities

The group velocity for the x mode near its cutoff frequency is well behaved, but that for the o mode near its cutoff frequency has some peculiar properties.

The group velocity is of the form

$$\mathbf{v}_g^\sigma = v_g^\sigma(\sin \theta_\sigma, 0, \cos \theta_\sigma), \quad (\text{A7})$$

where v_g^σ is the group speed and θ_σ is the angle between the ray direction and \mathbf{B} . The wave normal direction \mathbf{k} is at an angle θ to \mathbf{B} , which is along the z-axis and \mathbf{k} is in the x-z plane. One has

$$v_g^\sigma = \frac{n_\sigma c}{n_\sigma \partial(\omega n_\sigma) / \partial \omega} \sec(\theta - \theta_\sigma), \quad (\text{A8})$$

and it may be shown that one has (see e.g. Melrose 1980*b*; p. 261)

$$\tan(\theta - \theta_\sigma) = K_\sigma T_\sigma / (1 + T_\sigma^2), \quad (\text{A9})$$

$$K_\sigma = \frac{XY \sin \theta}{1 - X} \frac{T_\sigma}{T_\sigma - Y \cos \theta}. \quad (\text{A10})$$

For the x mode near its cutoff frequency at $1 - X = Y$, one finds $T_x = \cos \theta$, $K_x = \sin \theta$, $n_x \partial(\omega n_x) / \partial \omega = (2 - Y) / (1 - Y)(1 + \cos^2 \theta)$ and $\tan \theta_x = \frac{1}{2} \tan \theta$. Hence, one finds

$$\frac{v_g^x}{c} = n_x \frac{1 - Y}{2 - Y} (1 + 3 \cos^2 \theta)^{\frac{1}{2}} \quad (\text{A11})$$

near the cutoff frequency, with the ray direction between the wave normal direction and \mathbf{B} . The maximum deviation between the ray and the wave normal directions is for $\theta \approx 55^\circ$ when one has $\theta_x \approx 35^\circ$.

For the x mode the ray is at a smaller angle to \mathbf{B} than is the wave vector \mathbf{k} , and hence we are never concerned with rays nearly perpendicular to \mathbf{B} . The direction of grad Ω_e is close to the direction of \mathbf{B} near the magnetic pole, and hence for the x mode the angle between \mathbf{v}_g and grad Ω_e should never be close to $\frac{1}{2}\pi$. Neglecting the cosine of this angle can lead to errors only of order unity for the x mode.

The o mode near its cutoff frequency has a very strong dependence of n_o on θ . As $\omega - \omega_p$ approaches zero, n_o^2 approaches zero except for a range $\theta \lesssim \{2(\omega - \omega_p) / \Omega_e\}^{\frac{1}{2}}$; for $\theta = 0$, n_o^2 approaches $Y / (1 + Y)$. Except for $\theta \lesssim \{2(\omega - \omega_p) / \Omega_e\}^{\frac{1}{2}}$, one finds $T_o \approx \infty$, $\theta_o \approx \frac{1}{2}\pi$ and

$$v_g^o / c \approx n_o \sin \theta. \quad (\text{A12})$$

Thus the rays are directed nearly perpendicular to \mathbf{B} . In this range we may approximate the refractive index by

$$n_o^2 \approx (1 - X) / (1 - X \cos^2 \theta). \quad (\text{A13})$$

In the opposite limit $\theta \lesssim \{2(\omega - \omega_p) / \Omega_e\}^{\frac{1}{2}}$, the group velocity swings rapidly as a function of θ from $\theta_o \approx \frac{1}{2}\pi$ to $\theta_o = 0$ for $\theta = 0$ with $v_g^o / c \approx Y^{\frac{1}{2}}(1 + Y)^{3/2} / (1 + \frac{3}{2}Y + Y^2)$ at $\theta = 0$.

Over the range of relevance here we have, from (A12) and (A13) with $\omega - \omega_p \ll \omega_p$,

$$v_g^0/c \approx \{2(\omega - \omega_p)/\omega_p\}^{1/2}. \quad (\text{A14})$$

However, the very small values of v_g^0 allowed by (A14) are not obtained in practice because the region $\omega \approx \omega_p$ is kinematically forbidden by the requirements $v_c^2 \gg V^2 > 0$.

Note added in proof. In a recent paper Omidi *et al.* (1983) have remarked that the results of Omidi and Gurnett (1982) overestimate the growth in the lower band by more than an order of magnitude. Their revised results are consistent with those reported here.

Manuscript received 11 November 1982, accepted 17 May 1983

